J. Biochem. **135**, 663–671 (2004)
DOI: 10.1093/jb/mvh080

Mass Spectrometry on Hydrogen/Deuterium Exchange of Dihydrofolate Reductase: Effects of Ligand Binding

Tatsuya Yamamoto, Shunsuke Izumi and Kunihiko Gekko*

Department of Mathematical and Life Sciences, Graduate School of Science, Hiroshima University, Higashi-Hiroshima 739-8526

Received March 11, 2004; accepted March 31, 2004

To address the effects of ligand binding on the structural fluctuations of *Escherichia coli* dihydrofolate reductase (DHFR), the hydrogen/deuterium (H/D) exchange kinetics of its binary and ternary complexes formed with various ligands (folate, dihydrofolate, tetrahydrofolate, NADPH, $NADP^+$, and methotrexate) were examined using electrospray ionization mass spectrometry. The kinetic parameters of H/D exchange reactions, which consisted of two phases with fast and slow rates, were sensitively influenced by ligand binding, indicating that changes in the structural fluctuation of the DHFR molecule are associated with the alternating binding and release of the cofactor and substrate. No additivity was observed in the kinetic parameters between a ternary complex and its constitutive binary complexes, indicating that ligand binding cooperatively affects the structural fluctuation of the DHFR molecule via long-range interactions. The local H/D exchange profile of pepsin digestion fragments was determined by matrix-assisted laser desorption/ionization mass spectrometry, and the helix and loop regions that appear to participate in substrate binding, largely fluctuating in the apo-form, are dominantly influenced by ligand binding. These results demonstrate that the structural fluctuation of kinetic intermediates plays an important role in enzyme function, and that mass spectrometry on H/D exchange coupled with ligand binding and protease digestion provide new insight into the structure–fluctuation–function relationship of enzymes.

Key words: dihydrofolate reductase, hydrogen/deuterium exchange, ligand binding, mass spectrometry, structural fluctuation.

Abbreviations: CHCA, α-cyano-4-hydroxycinnamic acid; DHF, dihydrofolate; DHFR, dihydrofolate reductase; ESI, electrospray ionization; H/D, hydrogen/deuterium; MALDI, matrix-assisted laser desorption/ionization; MS, mass spectrometry; MTX, methotrexate; THF, tetrahydrofolate; TOF, time of flight.

What underlies the flexibility of an enzyme structure that allows it to adopt conformations suitable for binding a substrate and a cofactor? This is a basic problem in understanding the structure–function relationships of enzymes, but information in this area is limited despite many X-ray structural analyses of protein–ligand complexes (*1*, *2*). Dihydrofolate reductase from *Escherichia coli* (DHFR), a monomeric protein of 159 amino acids with no disulfide bonds, is an excellent enzyme for studying such ligand-mediated fluctuations, because its enzyme reaction involves various intermediates consisting of binary and ternary complexes of coenzyme and substrate that are large relative to its own size. The X-ray crystal structure of DHFR has been determined for the apo-enzyme (*3*) and for binary and ternary complexes formed with many ligands (*1*) (Fig. 1). High-pressure NMR has revealed the existence of active-site hinge motion involving the Met20 loop that might be directly relevant to function (*4*). The movie constructed by Sawaya and Kraut (*1*) suggests how the DHFR molecule actively and cooperatively fluctuates to accommodate the coenzyme and substrate. In previous studies (*5–7*), we found that mutations at Gly67, Gly121, and Ala145 in three independent loops that do not directly participate in catalytic reactions significantly affect the stability and function of DHFR. These results indicate that DHFR can assume highly fluctuating conformations in solution, the detailed knowledge of which may be crucial to understanding reaction mechanisms.

Among various experimental techniques for detecting protein dynamics (*8–11*), hydrogen/deuterium (H/D) exchange is a novel means for determining simultaneously the exchange rate and the number of protons involved (*12*, *13*). H/D exchange has been monitored mainly by infrared spectroscopy and NMR (*14–16*), but the recent developments of electrospray ionization mass spectrometry (ESI-MS) and matrix-assisted laser desorption/ionization mass spectrometry (MALDI-MS) have opened a new field in the investigation of H/D exchange in proteins (*17–19*), because the number of exchangeable protons can be determined rapidly and with an accuracy of 1.006 Da using only a small sample. We have recently applied MALDI-MS and ESI-MS to investigate structural fluctuations of DHFR, and found that investigating H/D exchange coupled with protease digestion and amino acid substitution provide useful information on the overall and local structural fluctuations of this enzyme (*20*, *21*). The mechanisms underlying the flexibility of kinetic intermediates in the enzyme reaction are yet to be elucidated.

*To whom correspondence should be addressed. Fax: +81-82-424-7387, E-mail: gekko@sci.hiroshima-u.ac.jp

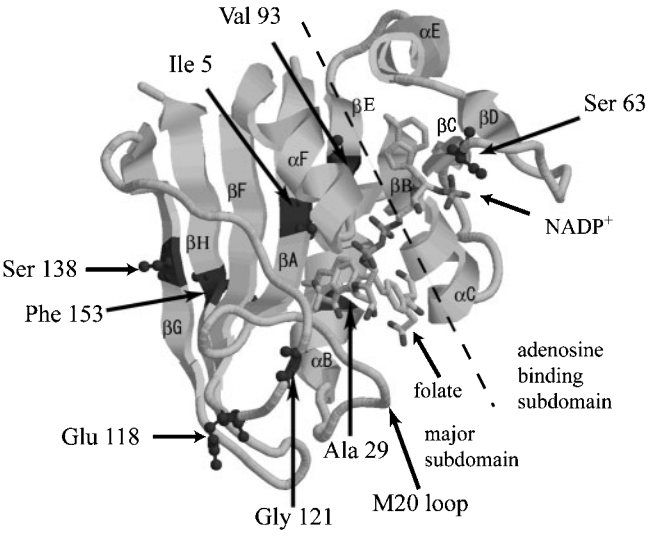

Fig. 1. **Three-dimensional X-ray structure of a DHFR–NAPD+–FOL ternary complex (PDBID: 1RA2) (*1*).** Residues except for Gly121 indicated by arrows are pepsin-digestion positions. The dashed line indicates an assumed boundary between two subdomains.

From these viewpoints, we examined the H/D exchange kinetics of the binary and ternary complexes of DHFR with various ligands [folate (FOL), dihydrofolate (DHF), tetrahydrofolate (THF), NADPH, NADP+, and methotrexate (MTX)] by means of ESI-MS. The H/D exchange kinetics of pepsin digestion fragments were also investigated by MALDI-MS. The effects of ligand binding on the structural fluctuations of this enzyme are discussed here in relation to enzyme function on the basis of the kinetic parameters of the H/D exchange reaction.

MATERIALS AND METHODS

Materials—The DHFR gene was prepared with overexpression plasmid pTP64-1 (5.3 kb) (*22*). The DHFR protein obtained from *E. coli* strain HB101 was purified on a MTX-agarose affinity column. The DHFR was fully dialyzed against 10 mM phosphate buffer (pH 7.0) containing 0.1 mM EDTA and 0.1 mM dithiothreitol at 4°C. For mass spectrometry, the DHFR solutions were finally dialyzed against 1 mM ammonium acetate. The concentration of DHFR was determined by measuring the absorption on a spectrophotometer (JASCO V-560) using a molar extinction coefficient of 31,100 M^{-1} cm^{-1} at 280 nm (*23*). Pepsin was obtained from Sigma, and D_2O (99.9% atomic D) and acetic acid-*d* (99% atomic D) were purchased from EURISO-TOP and IsoTec (USA), respectively. DHF, THF, NADP+, NADPH, and MTX were purchased from Sigma, and FOL from Katayama Kagaku Kogyo. All other chemicals were of analytical grade. The concentrations of ligands in stock solutions were determined by absorption measurements using the following molar extinction coefficients: 27,000 M^{-1} cm^{-1} at 282 nm for FOL, 28,000 M^{-1} cm^{-1} at 282 nm for DHF, 28,000 M^{-1} cm^{-1} at 297 nm for THF, 6,200 M^{-1} cm^{-1} at 339 nm for NADPH, 18,000 M^{-1} cm^{-1} at 260 nm for NADP+, and 22,100 M^{-1} cm^{-1} at 302 nm for MTX (*23*, *24*). Each ligand was added in minimal excess to make a 1:1 complex with the enzyme, taking into consideration the dissociation constant of the ligand (*23*).

H/D Exchange of the Entire DHFR Molecule—The H/D exchange reactions of DHFR–ligand complexes were initiated by mixing 400 μl of D_2O with 40 μl of 0.2–0.5 mM DHFR stock solutions including various ligands (1 mM ammonium acetate, pH 7.0) in 1.5-ml centrifuge tubes with caps at 15°C. At given intervals (every minute in most cases) after starting the H/D exchange reaction, 8 μl of the reaction mixture was removed and quenched (pH 2.5) by adding 2 μl of 20% acetic acid with an H:D atomic ratio of 1:10. The quench time was defined as the H/D exchange time, *t*. The obtained solution was immediately injected into a mass spectrometer and the molecular mass of the protein was monitored as a function of time for 50 min. When the deuterium concentration in solution is high at constant pH and temperature, the exchange of each amide protons follows first-order kinetics (*12*). Therefore, the time course of H/D exchange was analyzed using the following equation that assumes the presence of two phases with different rate constants:

$$M_t = M_\infty - A_1 \exp(-k_{ex1}t) - A_2 \exp(-k_{ex2}t) \quad (1)$$

where M_t and M_∞ are the molecular weights at exchange times t and infinity, respectively; A is the number of exchangeable protons that can be detected during the exchanging time at each phase; k_{ex} is the apparent first-order rate constant of H/D exchange at each phase; and subscripts 1 and 2 indicate the fast and slow reaction phases, respectively. The observed k_{ex} value represents the mean of all the exchange rates of different amide, side-chain, and terminal-residue protons.

H/D Exchange of Peptic Fragments—The deuterized DHFR was digested with pepsin to investigate the H/D exchange of digestion fragments. At given intervals after starting the H/D exchange reaction, the reaction solution was quenched by adding 2 μl of 20% acetic acid at an H:D atomic ratio of 1:10, pH 2.4, and 0°C. The exchange of side-chain protons can also be completed by acid quenching. A 24 μl sample of the quenched DHFR solution with or without ligand was digested for 1.5 min at pH 2.4 and 0°C with 2 μl of a 0.1% pepsin solution (eight-fold molar ratio of DHFR to pepsin). Then, an aliquot of the digested sample solution was mixed with saturated α-cyano-4-hydroxycinnamic acid (CHCA) in 50% acetonitrile and 0.1% trifluoroacetic acid (H:D = 1:10), and loaded onto a MALDI sample plate at 7 Pa. Ten minutes after starting the H/D exchange, the plate was set up on a MALDI-TOF (time of flight)-MS at 10^{-5} Pa.

To compare the H/D exchange kinetics of digestion fragments consisting of different numbers of residues, the molecular weight of each fragment at exchange time t, M_t, was normalized to the exchanged fraction of amide protons, D_t, using the following equation:

$$D_t = \frac{M_t - M_{side\ chain}^{100\%}}{M_\infty^{theo} - M_{side\ chain}^{100\%}} \quad (2)$$

where M_∞^{theo} and $M_{side\ chain}^{100\%}$ are the theoretically calculated molecular weights of each fragment and its side chains, respectively, assuming a complete exchange of their protons to deuterium. D_t was determined using the centroid

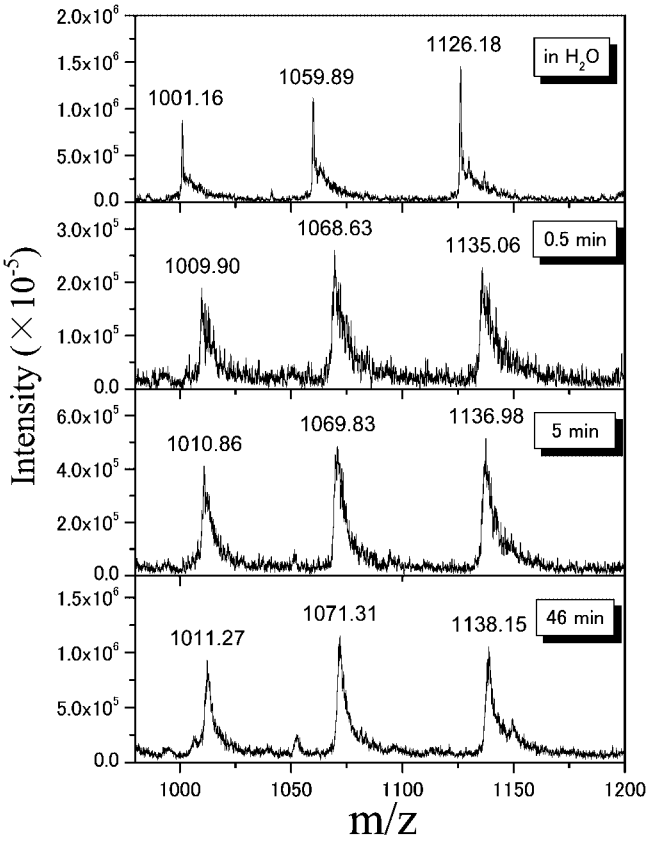

Fig. 2. **ESI mass spectra of the DHFR–NADPH complex formed with $[M+nH]^{+n}$ ions (n = 16, 17, and 18) at 0, 0.5, 5, and 46 min after the initiation of H/D exchange in D_2O.**

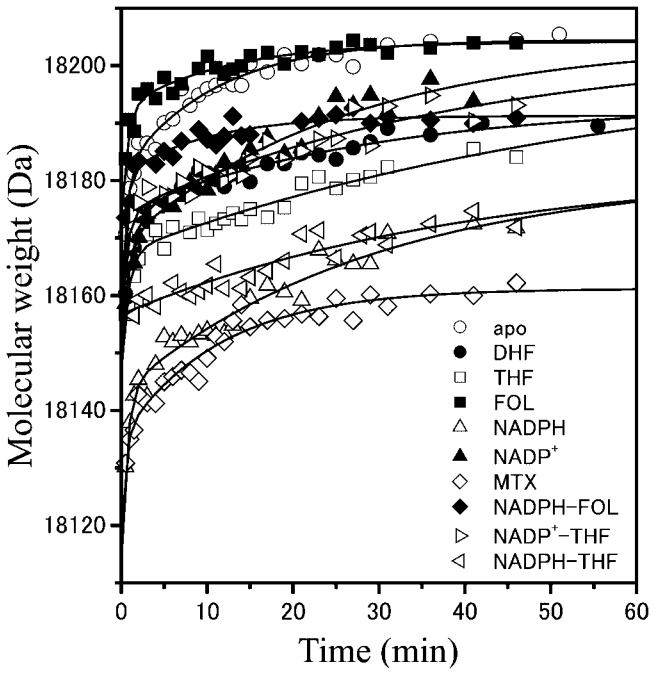

Fig. 3. **Plots of molecular weights of apo-DHFR and DHFR–ligand complexes against the H/D exchange time.**

mass of each isotopic distribution. The H/D exchange time course was analyzed using the following equation:

$$D_t = D_\infty - (D_\infty - D_0)\exp(-k_{\text{frag}}\, t) \quad (3)$$

where D_t, D_0, and D_∞ are the fractions of deuterium incorporation at exchange times of t, zero, and infinity, respectively; k_{frag} is the apparent first-order rate constant of the H/D exchange reaction of the fragment. The difference between D_∞ and D_0 is the fraction of exchangeable protons that can be detected during the exchange time. The observed k_{frag} value represents the average of all the exchange rates of the different amide protons. In order to clarify the contributions of α-helix, β-strand, and disordered forms to H/D exchange, D_t was decomposed into these three components by multiple regression analysis using the fractions of α-helix (f_α), β-strand (f_β), and disordered forms (f_d) in each of 17 fragments as independent variables:

$$D_t = D_{t,\alpha} f_\alpha + D_{t,\beta} f_\beta + D_{t,d} f_d \quad (4)$$

where $D_{t,\alpha}$, $D_{t,\beta}$, and $D_{t,d}$ represent the deuterium incorporations into the α-helix, β-strand, and disordered forms at time t, respectively.

Mass Spectrometry—The H/D exchange time course for DHFRs was examined with an electrospray ionization mass spectrometer (JMS-SX 102A, JEOL) equipped with an electrospray ion source (ESI10HS). Proteins were introduced into the electrospray ionization source at a rate of 0.2 ml·min^{-1} using a liquid chromatography pump. Protein ions were generated by ESI at a needle voltage of 2,000 V, and accelerated in the positive mode at 5,000 V. The temperature of the vaporizer was set to 180°C. The orifice, ring-electrode, and ion-guide voltages were 50, 150, and 4 V, respectively. The pressure in the analyzer was approximately 1×10^{-3} Pa.

The H/D exchange of peptic fragments was examined using MALDI-TOF-MS (Voyager RP-3, Perseptive Biosystems). Digestion fragments enclosed in CHCA crystals were ionized with an N_2 laser at 337 nm, and accelerated at an accelerating voltage of 25 kV and a pulse delay time of 300 ns.

RESULTS

Mass Spectra of DHFR–Ligand Complexes—Figure 2 shows mass spectra of DHFR–NADPH complexes with (positive) charges of +16, +17, and +18 in H_2O, and at 0.5, 5, and 46 min after mixing the DHFR solution with D_2O. All peaks shift to a larger m/z value and the peaks become narrower over time. Similar results were observed for all other DHFR–ligand complexes analyzed. All these spectra indicate the mass of the DHFR molecule without the ligand, since the ligand is released when H/D exchange is quenched by adding acetic acid. In this study, we analyzed the H/D exchange kinetics of DHFR–ligand complexes using the smallest centroid masses of the isotopic envelopes in the respective charge peak from +14 to +18 to eliminate the effects of the adduction of other small molecules.

H/D Exchange Kinetics—Figure 3 shows plots of the molecular weights of apo-DHFR and its binary and ternary complexes formed with various ligands (DHF, THF,

Table 1. **H/D exchange parameters of apo- and ligand-bound DHFRs.**[a]

Ligand	M_0 (Da)	M_∞ (Da)	A_1 (Da)	k_{ex1} (min^{-1})	A_2 (Da)	k_{ex2} (min^{-1})	ΔM_0 (Da)	ΔM_∞ (Da)
apo	18,152.2	18,204.5 ± 0.9	29.1 ± 9.9	1.81 ± 0.72	23.2 ± 1.6	0.09 ± 0.01	153.0	46.2
DHF	18,152.3	18,193.2 ± 3.1	22.0 ± 3.0	0.85 ± 0.21	18.9 ± 2.3	0.04 ± 0.01	153.2	57.5
THF	18,147.3	18,201.5 ± 16.9	20.1 ± 5.4	1.26 ± 0.45	34.1 ± 16.0	0.02 ± 0.01	148.1	49.2
FOL	18,173.9	18,204.2 ± 1.0	18.5 ± 6.5	1.47 ± 0.72	11.8 ± 1.6	0.08 ± 0.03	174.7	46.6
NADPH	18,113.9	18,181.2 ± 6.6	29.3 ± 10.5	1.52 ± 0.66	37.9 ± 5.4	0.03 ± 0.01	114.7	69.5
NADP$^+$	18,146.7	18,204.1 ± 6.0	22.1 ± 9.6	1.50 ± 0.81	35.3 ± 4.7	0.04 ± 0.01	147.6	46.6
MTX	18,118.9	18,161.2 ± 1.3	16.4 ± 18.5	2.10 ± 2.38	25.9 ± 1.9	0.09 ± 0.02	119.7	89.5
FOL-NADPH	18,161.3	18,191.3 ± 0.8	19.5 ± 8.8	1.73 ± 1.05	10.5 ± 2.1	0.10 ± 0.04	162.1	59.4
THF-NADP$^+$	18,155.4	18,202.8 ± 10.4	18.7 ± 10.5	1.52 ± 1.01	28.7 ± 9.2	0.03 ± 0.02	156.3	47.9
THF-NADPH	18,156.7	18,182.5 ± 8.7	–	–	25.8 ± 8.1	0.02 ± 0.01	157.5	68.3

[a] M_0 (= $M_\infty - A_1 - A_2$) and M_∞ are the molecular weight at t = 0 and ∞, respectively. A_1 and A_2 are the number of exchangeable protons in fast and slow reaction phases, respectively. k_{ex1} and k_{ex2} are the apparent first-order rate constant of H/D exchange in fast and slow reaction phases, respectively. ΔM_0 is the difference between M_0 and the molecular weight of apo-DHFR in H_2O (17,999.2 Da). ΔM_∞ (= $M_\infty^{theo} - M_\infty$) is the number of protected protons at t = ∞.

FOL, NADPH, NADP$^+$, MTX, NADPH–FOL, NADP$^+$–THF, and NADPH–THF) as a function of deuterium exchange time. All of the time courses, except that of the DHFR–NADPH–THF complex, appear to involve two phases with fast and slow exchange rates, rather than being single exponential, during the experimentally observed time interval. The data points satisfactorily fit the theoretical lines calculated by the least-squares regression analysis using Eq. 1, as also confirmed by residual-plot analysis (data not shown). The fast phase for the DHFR–NADPH–THF complex could not be observed, so its time course was analyzed assuming a single exponential phase with a slow exchange rate. The kinetic parameters calculated (M_∞, A_1, A_2, k_{ex1}, and k_{ex2}) are listed in Table 1 with the molecular weight at t = 0, M_0, which is defined as the difference between M_∞ and (A_1 + A_2). In this table, ΔM_0 is the difference between M_0 and the molecular weight of apo-DHFR (M_w = 17999.2 Da) in H_2O, which refers to the number of very fast exchangeable protons exchanged at t = 0, with most of the side-chain protons being involved in this phase. ΔM_∞ (= $M_\infty^{theo} - M_\infty$) in the last column of Table 1 is the difference between M_∞ and the theoretical molecular weight for maximum deuterium incorporation, M_∞^{theo}, which was calculated by considering the number of exchangeable protons in each complex and the H:D atomic ratio (1:10) in the reaction medium. ΔM_∞ indicates the number of amide protons protected from deuterium exchange at t = ∞ due to the limited flexibility of the secondary and tertiary structures of the protein.

Each complex exhibits significant changes in k_{ex1} (0.85–2.10 min^{-1}), k_{ex2} (0.02–0.10 min^{-1}), A_1 (16.4–29.3 Da), A_2 (10.5–37.9 Da), ΔM_0 (114.7–174.7 Da), and ΔM_∞ (46.2–89.5 Da) relative to the corresponding values for the apo-enzyme: k_{ex1} (1.81 min^{-1}), k_{ex2} (0.09 min^{-1}), A_1 (29.1 Da), A_2 (23.2 Da), ΔM_0 (153.0 Da), and ΔM_∞ (46.2 Da). These results indicate that structural fluctuations of the DHFR molecule are significantly influenced by ligand binding.

H/D Exchange of Peptic Fragments of DHFR–Ligand Complexes—In a previous study, we developed a method for assigning segment-specific H/D exchange kinetics by MALDI-TOF-MS coupled with pepsin digestion (*20*). This method was applied to evaluate the effects of ligand binding on the segment-specific H/D exchange of DHFR. The binary and ternary complexes of DHFR formed with NADPH and NADPH–FOL were digested with pepsin after H/D exchange, and 17 digestion fragments covering almost the entire sequence of DHFR were identified: residues 1–17, 5–28, 9–28, 9–30, 29–62, 31–62, 63–81, 63–92, 93–110, 93–117, 93–118, 93–137, 111–137, 118–137, 138–152, 138–153, and 153–159. Figure 4 shows the time courses of H/D exchange of some digestion fragments of apo-DHFR and its complexes formed with NADPH and NADPH–FOL. It is clear that all fragments exhibit an exponential time course during the examined time interval, and that the least-squares regression lines calculated using Eq. 3 fit the data points satisfactorily. Similar results were also obtained for the other fragments. The kinetic parameters (D_∞, D_0, and k_{frag}) calculated for the complexes formed with NADPH and NADPH–FOL are listed in Tables 2 and 3, respectively. The molecular weight, M_w, of each fragment in H_2O and the theoretical molecular weight for maximum deuterium incorporation, M_∞^{theo}, at an H:D ratio of 1:10 are listed in the third and

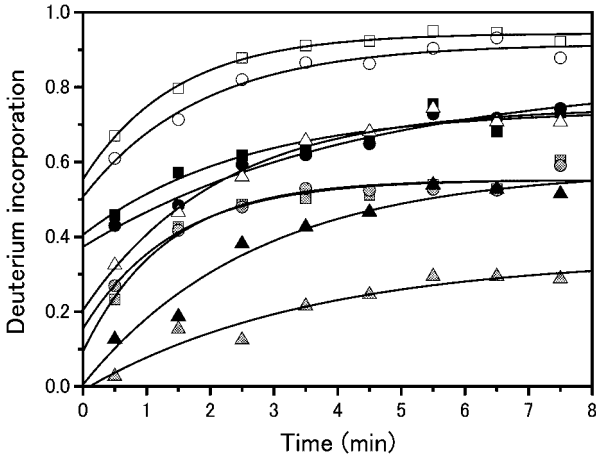

Fig. 4. **Time course of deuterium incorporation of peptic fragments of apo-type DHFR, DHFR–NADPH, and DHFR–NADPH–FOL complexes.** Symbols refer to fragments 5–28 (squares), 118–137 (circles), and 153–159 (triangles) in the apo-type DHFR (white), DHFR–NADPH (gray), and DHFR–NADPH–FOL (black) complexes. Solid lines show least-squares regressions calculated using Eq. 3.

Table 2. **H/D exchange kinetics parameters of peptic fragments of the DHFR–NADPH complex.**[a]

No.	Residue	M_w (Da)	M_∞^{theo} (Da)	D_∞	D_0	$D_\infty - D_0$	k_{frag} (min^{-1})
1	1– 17	1,802.21	1,825.99	0.44 ± 0.02	0.00	0.44 ± 0.05	0.54 ± 0.14
2	5– 28	2,581.02	2,613.95	0.55 ± 0.02	0.09	0.46 ± 0.07	0.77 ± 0.21
3	9– 28	2,212.55	2,241.82	0.57 ± 0.03	0.14	0.43 ± 0.07	0.64 ± 0.22
4	9– 30	2,469.84	2,501.85	0.52 ± 0.02	0.09	0.43 ± 0.05	0.64 ± 0.17
5	29– 62	4,000.72	4,062.93	0.50 ± 0.02	0.09	0.41 ± 0.06	0.72 ± 0.20
6	31– 62	3,743.44	3,802.90	0.45 ± 0.02	0.04	0.41 ± 0.07	0.87 ± 0.24
7	63– 81	2,077.17	2,111.93	0.56 ± 0.04	0.23	0.33 ± 0.03	0.26 ± 0.07
8	63– 92	3,177.48	3,224.13	0.56 ± 0.03	0.20	0.36 ± 0.04	0.41 ± 0.13
9	93–110	2,003.35	2,033.54	0.53 ± 0.02	0.18	0.35 ± 0.03	0.51 ± 0.12
10	93–117	2,817.24	2,857.49	0.49 ± 0.03	0.14	0.34 ± 0.04	0.40 ± 0.13
11	93–118	2,946.36	2,988.44	0.53 ± 0.03	0.18	0.35 ± 0.04	0.44 ± 0.14
12	93–137	5,212.64	5,281.25	–	–	–	–
13	111–137	3,227.31	3,267.56	0.56 ± 0.01	0.18	0.39 ± 0.03	0.61 ± 0.11
14	118–137	2,413.42	2,443.60	0.55 ± 0.02	0.15	0.40 ± 0.05	0.69 ± 0.16
15	138–152	1,710.69	1,739.05	0.57 ± 0.04	0.28	0.29 ± 0.03	0.34 ± 0.13
16	138–153	1,857.87	1,887.14	0.55 ± 0.02	0.20	0.35 ± 0.03	0.46 ± 0.10
17	153–159	962.10	979.48	0.35 ± 0.07	–0.01	0.36 ± 0.05	0.28 ± 0.14
18	1–159	17,999.2	18,250.7	0.54 ± 0.04	0.11	0.44 ± 0.04	0.40 ± 0.15

[a] M_w, molecular weight of fragments digested by pepsin in H_2O; M_∞^{theo}, molecular weight calculated for the maximum deuterium incorporation in D_2O; D_0 and D_∞, deuterium incorporations at $t = 0$ and $t = \infty$, respectively; k_{frag}, apparent first-order rate constant of the H/D exchange reaction.

Table 3. **H/D exchange kinetics parameters of peptic fragments of DHFR–FOL–NADPH complex.**

No.	Residue	M_w (Da)	M_∞^{theo} (Da)	D_∞	D_0	$D_\infty - D_0$	k_{frag} (min^{-1})
1	1– 17	1,802.21	1,825.99	0.56 ± 0.04	0.22	0.34 ± 0.04	0.38 ± 0.16
2	5– 28	2,581.02	2,613.95	0.74 ± 0.04	0.41	0.33 ± 0.05	0.40 ± 0.17
3	9– 28	2,212.55	2,241.82	0.75 ± 0.04	0.43	0.32 ± 0.04	0.37 ± 0.14
4	9– 30	2,469.84	2,501.85	0.68 ± 0.04	0.34	0.35 ± 0.06	0.48 ± 0.22
5	29– 62	4,000.72	4,062.93	0.69 ± 0.07	0.32	0.37 ± 0.05	0.26 ± 0.12
6	31– 62	3,743.44	3,802.90	0.73 ± 0.09	0.33	0.40 ± 0.08	0.21 ± 0.11
7	63– 81	2,077.17	2,111.93	0.75 ± 0.09	0.32	0.42 ± 0.08	0.23 ± 0.12
8	63– 92	3,177.48	3,224.13	0.72 ± 0.02	0.40	0.32 ± 0.02	0.34 ± 0.07
9	93–110	2,003.35	2,033.54	–	–	–	–
10	93–117	2,817.24	2,857.49	0.61 ± 0.04	0.26	0.35 ± 0.04	0.32 ± 0.12
11	93–118	2,946.36	2,988.44	0.77 ± 0.11	0.37	0.39 ± 0.09	0.22 ± 0.14
12	93–137	5,212.64	5,281.25	0.65 ± 0.03	0.25	0.40 ± 0.06	0.54 ± 0.19
13	111–137	3,227.31	3,267.56	0.74 ± 0.02	0.34	0.40 ± 0.03	0.44 ± 0.10
14	118–137	2,413.42	2,443.60	0.83 ± 0.07	0.37	0.46 ± 0.05	0.23 ± 0.08
15	138–152	1,710.69	1,739.05	0.76 ± 0.04	0.33	0.43 ± 0.04	0.37 ± 0.11
16	138–153	1,857.87	1,887.14	0.71 ± 0.03	0.29	0.42 ± 0.03	0.39 ± 0.10
17	153–159	962.10	979.48	0.58 ± 0.05	0.00	0.57 ± 0.05	0.37 ± 0.12
18	1–159	17,999.2	18,250.7	0.63 ± 0.07	0.24	0.39 ± 0.06	0.33 ± 0.18

fourth columns of each table, respectively. The fraction of deuterium incorporation at $t = 0$, D_0, is listed in the sixth column of the tables.

DISCUSSION

Effects of Ligand Binding on H/D Exchange Kinetics—As shown in Table 1, ligand binding clearly affects the H/D exchange kinetic parameters of DHFR. The parameters ΔM_0, A_1, A_2, and ΔM_∞ for apo-DHFR and its complexes formed with various ligands are indicated by bars in Fig. 5 to allow their easy comparison. At present, the protons corresponding to these four masses are not explicitly attributed to locations in the structure, but it is pertinent to discuss the characteristic effects of the ligands. The ΔM_∞ value of apo-DHFR is lower than or equal to that of all the other complexes, suggesting that ligand binding reduces the structural fluctuation, and that its effects extend to the internal residues of the protein molecule or secondary structures whose amide protons are not susceptible to deuterium exchange. NADPH and NADPH–THF have large depression effects, and a strong inhibitor of this enzyme, MTX, exerts the most significant effect among the ligands examined. It is noteworthy that such a large increase in ΔM_∞ is not observed for $NADP^+$, the oxidized form of NADPH. The ΔM_∞ value for NADPH–THF is also larger than that for $NADP^+$–THF, indicating that the introduction of positive valency by the oxidation of NADPH induces large fluctuations in the DHFR molecule. Another noticeable point is that there is no additivity in ΔM_∞ values between a ternary complex and its constitutive binary complexes: the difference in ΔM_∞ values between DHFR–NADPH–FOL and apo-DHFR, 13.2 Da (= 59.4 – 46.2), is smaller than the sum of

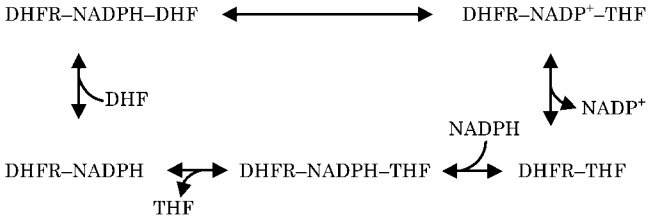

Scheme 1.

differences in ΔM_∞ values produced when DHFR independently binds FOL and NADPH, 23.7 Da [= (46.6 – 46.2) + (69.5 – 46.2)]. These results suggest that ligand binding cooperatively affects the structural fluctuation of the DHFR molecule via long-range interactions.

The ΔM_0 values of most complexes, except NADPH, FOL, and MTX, are close to that of apo-DHFR, indicating that ligand binding has only a small effect on fast-exchangeable protons around the protein surface. The significantly lower value of ΔM_0 for NADPH and MTX, consistent with the larger value of ΔM_∞, indicates reduced fluctuations in DHFR. It is interesting that FOL significantly increases ΔM_0 since ligand binding is generally expected to cause depressed fluctuation. The reason for this discrepancy is not clear, but the fluctuation of the flexible region may be more effectively enhanced as ΔM_∞ is not affected. The effects of ligands on A_1 and A_2 cannot be discussed quantitatively at present because the boundary between the two phases is not clearly distinguishable, but most of A_1 would be ascribed to amide protons with a slower exchange rate around the molecular surface since a good correlation (r = 0.84) exists between A_1 and the accessible surface area as calculated from the X-ray structure (*25*) (data not shown).

The H/D exchange kinetics of a protein have been explained by the following local unfolding model (*12*, *13*):

$$\mathrm{N(H)} \underset{k_f}{\overset{k_u}{\rightleftharpoons}} \mathrm{O(H)} \overset{k_c}{\rightarrow} \mathrm{O(D)} \qquad (5)$$

where 'N' represents the folded state of a protein; 'O' is a partially unfolded open state in which the exchangeable

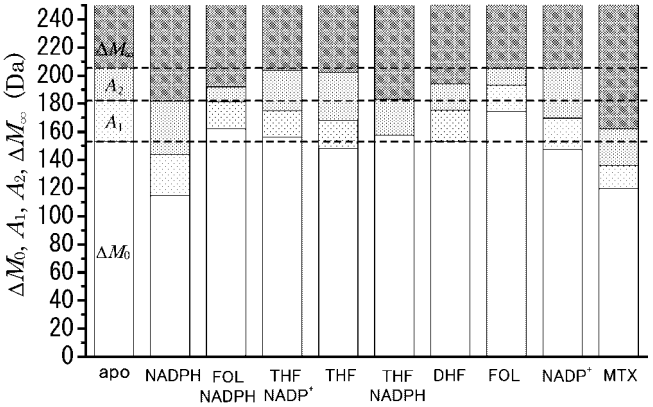

Fig. 5. **H/D exchange mass profiles of apo-DHFR and DHFR–ligand complexes.** Broken lines show the mass levels for apo-DHFR.

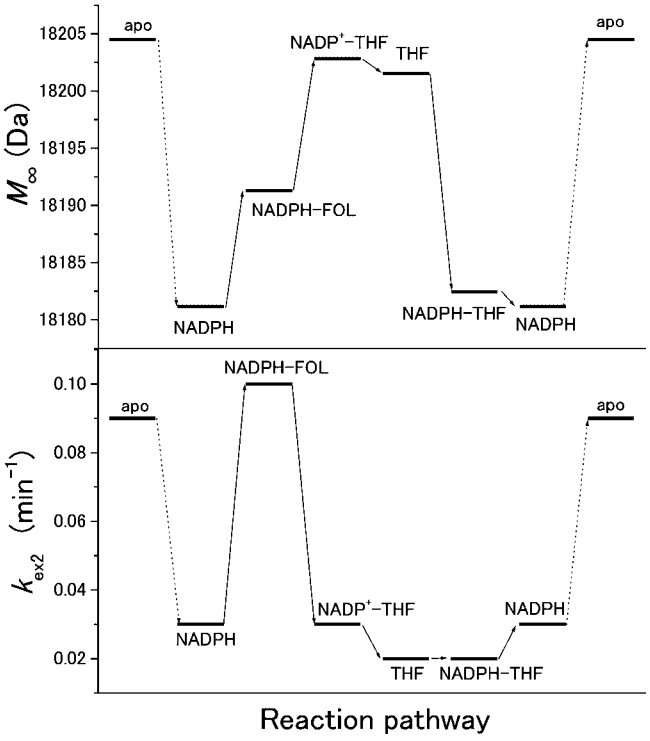

Fig. 6. **M_∞ and k_{ex2} of the kinetic intermediates as a function of the reaction pathway.**

protons are exposed to the solvent; and k_u, k_f, and k_c are the rate constants for the individual processes. When $k_c > k_f$, the observed rate of exchange, k_{ex}, is determined by the rate of opening of the protein structure, k_u (EX_1 mechanism). If $k_c < k_f$, the observed rate of exchange is $(k_u/k_f)k_c$, and then k_{ex} is proportional to the equilibrium constant for the local unfolding process (EX_2 mechanism). The H/D exchange of proteins follows the EX_2 mechanism under most conditions, with an EX_1 mechanism being observed only under the conditions where H/D exchange is intrinsically very rapid and no longer rate-limiting (*12*, *26*). In a previous paper (*20*), we found that the H/D exchange reaction of wild-type DHFR is dominated by an EX_2 mechanism under the experimental conditions used (neutral pH).

In the present system, the reaction N(H) ↔ O(H) in Eq. 5 consists of two processes with different rate constants: k_{ex1} and k_{ex2}. From the k_{ex1} and k_{ex2} values, the changes in Gibbs free energy (ΔG_{ex}) for the corresponding two processes, ΔG_{ex1} and ΔG_{ex2}, of apo-DHFR are estimated to be 14.8 and 22.0 kJ·mol^{-1}, respectively. In this calculation, k_c was assumed to be 879.4 min^{-1}, as determined for a model peptide at pH 5–8 (*26*). Since k_c would not be dependent on ligands, the difference in ΔG_{ex} between apo-DHFR and each complex, $\Delta\Delta G_{ex}$, can be calculated from

$$\begin{aligned}\Delta\Delta G_{ex} &= \Delta G_{ex}\,(\mathrm{complex}) - \Delta G_{ex}\,(\mathrm{apo}) \\ &= -RT \ln [(k_u/k_f)^{\mathrm{complex}}/(k_u/k_f)^{\mathrm{apo}}]\end{aligned} \qquad (6)$$

Thus we can estimate that $\Delta\Delta G_{ex1}$ ranges from –0.37 (MTX) to 1.83 (DHF) kJ·mol^{-1} and that $\Delta\Delta G_{ex2}$ ranges from –0.26 (NADPH–FOL) to 3.72 (THF and NADPH–

Table 4. **Deuterium incorporation (D_∞) of secondary structures and multiple correlation coefficients (r^2).**

Ligand	D_∞			r^2
	α-helix	β-strand	Disordered	
apo	0.87	0.75	0.97	0.98
NADPH	0.61	0.36	0.57	0.92
NADPH-FOL	0.75	0.57	0.74	0.88

THF) kJ·mol^{-1}, depending on the ligands. These values amount to at most 12% and 17% of ΔG_{ex1} and ΔG_{ex2}, respectively, suggesting that ligand binding would cause energetically large perturbations in the structural fluctuations even though these ligands represent only a few percent of the size of the DHFR molecule. There is also no additivity in $\Delta\Delta G_{ex}$ between a ternary complex and its constitutive binary complexes, indicating that the effect of ligand binding extends cooperatively over the DHFR molecule.

H/D Exchange–Function Relationship—DHFR catalyzes the NADPH-linked reduction of DHF to THF. The reaction pathway is known to cycle through five intermediate states (DHFR–NADPH, DHFR–NADPH–DHF, DHFR–NADP$^+$–THF, DHFR–THF, and DHFR–NADPH–THF) that involve some equilibrium states, such as DHFR–NADP$^+$ (Scheme 1) (*23*).

In the cycle shown in Scheme 1, the ternary complex DHFR–NADPH–DHF exists only transiently because the hydride transfer from NADPH to DHF is very rapid. The movie simulation produced by Sawaya and Kraut (*1*) suggests that DHFR is actively and cooperatively fluctuating on binding and releasing these ligands. Elucidating the H/D exchange properties of these intermediates would be helpful for understanding how the enzyme reaction is linked to the conformational flexibility.

Figure 6 shows the changes in M_∞ and k_{ex2} according to the reaction coordinate, for which we assumed a complex DHFR–NADPH–FOL for the transient state DHFR–NADPH–DHF, because the life-time of DHFR–NADPH–DHF is too short to investigate its H/D exchange by the present method and the DHFR complexes formed with both ligands have very similar X-ray structures (*1*). The binding of NADPH (the initial step of the enzyme reaction) decreases M_∞ and k_{ex2}, indicating reduced structural fluctuations of DHFR. The binding of DHF also decreases M_∞ and k_{ex2}, but the ternary complex DHFR–NADPH–FOL shows the largest k_{ex2}, suggesting that the transient state is the most kinetically flexible of the intermediates. This is also expected from the largest values of M_0 and k_{ex1} in the intermediates (Table 1). Such a large fluctuation of the transient state would be necessary for DHFR to simultaneously accommodate a coenzyme and substrate that are large relative to its own size. The enhanced fluctuation of the transient state is significantly diminished by the hydride transfer from NADPH to DHF, which accompanies an increase in the exchangeable protons (M_∞). The produced ternary complex, DHFR–NADPH–THF, is expected to be the most rigid of the intermediates. Thus the profiles of M_∞ and k_{ex2} reveal that the structural fluctuation of the DHFR molecule is changed dramatically by the uptake and release of coenzyme and substrate. Similar changes were also found in volume fluctuations in this reaction pathway, as monitored by adiabatic compressibility (*25*). Since the compressibility changes are mainly determined by the characteristics of internal cavities, the observed H/D exchange profile in the intermediates may reflect changes in the compactness of the DHFR molecule induced by ligand binding. The inconsistent changes between M_∞ and k_{ex2} in the reaction pathway suggest that the large spacial fluctuations are not necessarily rapid.

H/D Exchange of Peptic Fragments—To address the effects of ligand binding on the local fluctuation of the DHFR molecule, the deuterium incorporations of peptic fragments of two complexes, DHFR–NADPH and DHFR–NADPH–FOL, were compared with that of apo-DHFR as published previously (*20*). As shown in Table 2, peptic fragments of the DHFR–NADPH complex induce significant changes in k_{ex} (0.26–0.87 min^{-1}), D_0 (–0.01–0.28), and D_∞ (0.35–0.57) from the corresponding values for the whole DHFR molecule: k_{ex} = 0.40 min^{-1}, D_0 = 0.11, and D_∞ = 0.54. Peptic fragments of the ternary complex DHFR–

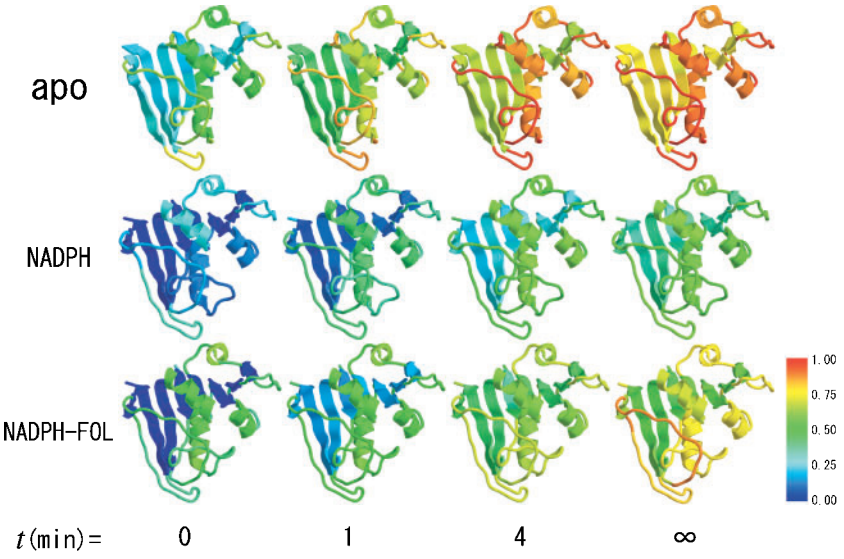

Fig. 7. **Fluctuation maps of apo-DHFR, DHFR–NADPH, and DHFR–NADPH–FOL complexes at different H/D exchange times.** The colors of the segments correspond to the proportion of deuterium incorporation trisected with H/D exchange parameters at each exchange time.

NADPH–FOL also show large changes in k_{ex} (0.21–0.54 min^{-1}), D_0 (0.00–0.43), and D_∞ (0.56–0.83) from the corresponding values for the whole DHFR molecule: k_{ex} = 0.33 min^{-1}, D_0 = 0.24, and D_∞ = 0.63 (Table 3). These results indicate that the fluctuation of each fragment, as well as that of the whole DHFR molecule, is significantly influenced by ligand binding: the fluctuation of some fragments is enhanced whereas that of other fragments is reduced compared with the overall fluctuation of the protein molecule.

The H/D exchange kinetic parameters of digestion fragments were used to assign the fluctuations of the secondary structure units. The deuterium incorporation of each fragment at a given exchange time t (D_t) was decomposed into three contributions from α-helix, β-strand, and disordered forms by multiple regression analysis using Eq. 4. The secondary structure contents of DHFR–NADPH and DHFR–NADPH–FOL complexes were calculated from PDBID: 1RA1 and 1RX3, respectively (*1*). The D_∞ values of α-helix ($D_{\infty,\alpha}$), β-strand ($D_{\infty,\beta}$), and disordered forms ($D_{\infty,d}$) at $t = \infty$ are listed in Table 4 together with those of apo-DHFR. Evidently, all parameters of the complexes are smaller than those of apo-DHFR: the H/D exchange of three secondary structures decreases in the order of apo-DHFR > DHFR–NADPH–FOL > DHFR–NADPH. It is seen that H/D exchange is most strongly reduced in β-strand regions, independent of the ligands, whereas both α-helix and disordered forms maintain a high level of deuterium incorporation.

To visualize the effects of ligand binding on the local fluctuations of apo-DHFR, DHFR–NADPH, and DHFR–NADPH–FOL, the deuterium incorporation (D_t) of the individual secondary structures at t = 0, 1, 4, and ∞ min is mapped with different colors in Fig. 7. Evidently, the helix and loop regions participating in substrate binding (Met20 loop, αB, αB-βB loop, αC, and αC-βC loop) are very flexible in apo-DFHR, but their fluctuation is reduced by the binding of NADPH and FOL. The fluctuation of the four helices appears to increase in the order αB ≃ αC > αF > αE in apo-DHFR (*20*), but this order changes to αE > αB > αC > αF for DHFR–NADPH–FOL, while no significant difference in fluctuation of the four helices is observed for DHFR–NADPH. These results are evidence that fluctuation of these helices regulates the accommodation of coenzyme and substrate. High deuterium incorporation is also seen for the βF-βG loop in DHFR–NADPH–FOL. This is consistent with findings that fluctuations of this loop, which is not included in any binding site for coenzyme and substrate, is important for enzyme function. We found that a single amino acid substitution at site 121 on the βF-βG loop does not affect substrate binding (K_m), but significantly decreases the catalytic rate (k_{cat}) (*5*). Benkovic and coworkers (*27–29*) proposed that the coupled movement between the βF-βG and Met20 loops, as demonstrated by Sawaya and Kraut (*1*), affects hydride transfer from NADPH to DHF. Thus, these fluctuation maps obtained from H/D exchange parameters of peptic fragments can be used to visualize characteristic ligand-induced changes in the local fluctuations of a DHFR molecule.

The present study reveals that the kinetic parameters of the H/D exchange reaction of DHFR are sensitively influenced by ligand binding, which indicates that structural fluctuations of the intermediates in the reaction pathway play an important role in enzyme function. The contribution of helix and loop regions to enzyme function can be derived from the local fluctuation map of digestion fragments. Our results demonstrate that mass spectrometry on H/D exchange coupled with protease digestion is a powerful tool for characterizing ligand-induced changes in the fluctuation of a protein molecule that are closely related to enzyme function.

We thank Professor Tsutomu Masujima of Hiroshima University for providing MALDI-TOF-MS facilities. We also thank the Instrument Center for Chemical Analysis, Hiroshima University, for measurements of ESI double-focusing mass spectra, and the Faculty of Applied Biological Sciences, Hiroshima University, for providing ESI-QIT-MS/MS facilities. This work was supported by a Grant-in-Aid for Scientific Research (No. 12480201) from the Ministry of Education, Science, Sports and Culture of Japan.

REFERENCES

1. Sawaya, M.R. and Kraut, J. (1997) Loop and subdomain movements in the mechanism of *Escherichia coli* dihydrofolate reductase: crystallographic evidence. *Biochemistry* **36**, 586–603
2. Lumry, R. (1995) The new paradigm for protein research in *Protein-Solvent Interactions* (Gregory, R.B., ed.) , pp. 1–141, Marcel Dekker, New York
3. Bystroff, C. and Kraut, J. (1991) Crystal structure of unliganded *Escherichia coli* dihydrofolate reductase. Ligand-induced conformational changes and cooperativity in binding. *Biochemistry* **30**, 2227–2239
4. Kitahara, R., Sareth, S., Yamada, H., Ohmae, E., Gekko, K., and Akasaka, K. (2000) High pressure NMR reveals active-site hinge motion of folate-bound *Escherichia coli* dihydrofolate reductase. *Biochemistry* **39**, 12789–12795
5. Gekko, K., Kunori, Y., Takeuchi, H., Ichihara, S., and Kodama, M. (1994) Point mutations at glycine-121 of *Escherichia coli* dihydrofolate reductase: important roles of a flexible loop in the stability and function. *J. Biochem.* **116**, 34–41
6. Ohmae, E., Iriyama, K., Ichihara, S., and Gekko, K. (1996) Effects of point mutations at the flexible loop glycine-67 of *Escherichia coli* dihydrofolate reductase on its stability and function. *J. Biochem.* **119**, 703–710
7. Ohmae, E., Ishimura, K., Iwakura, M., and Gekko, K. (1998) Effects of point mutations at the flexible loop alanine-145 of *Escherichia coli* dihydrofolate reductase on its stability and function. *J. Biochem.* **123**, 839–884
8. Karplus, M. and McCammon, J.A. (1981) The internal dynamics of globular proteins. *CRC Crit. Rev. Biochem.* **9**, 293–349.
9. Gekko, K. and Hasegawa, Y. (1986) Compressibility-structure relationship of globular proteins. *Biochemistry* **25**, 6563–6571
10. Wüthrich, K. (1990) Structure and dynamics in proteins of pharmacological interest. *Biochem. Pharmacol.* **40**, 55–62
11. Creighton, T. (1993) *Proteins: Structure and Molecular Properties*. Freeman and Company, New York
12. Hvidt, A. and Nielsen, S.O. (1966) Hydrogen exchange in proteins. *Adv. Protein Chem.* **21**, 287–386
13. Englander, S.W. and Kallenbach, N.R. (1983) Hydrogen exchange and structural dynamics of proteins and nucleic acids. *Q. Rev. Biophys.* **16**, 521–655
14. Nakanishi, M. and Tsuboi, M. (1976) Structure and fluctuation of a *Streptomyces* subtilisin inhibitor. *Biochim. Biophys. Acta* **434**, 365–376
15. Wagner, G. and Wüthrich, K. (1982) Amide proton exchange and surface conformation of the basic pancreatic trypsin inhibitor in solution. Studies with two-dimensional nuclear magnetic resonance. *J. Mol. Biol.* **160**, 343–361

16. Akasaka, K., Inoue, T., Hatano, H., and Woodward, C.K. (1985) Hydrogen exchange kinetics of core peptide protons in *Streptomyces* subtilisin inhibitor. *Biochemistry* **24**, 2973–2979
17. Fenn, J.B., Mann, M., Meng, C.K., Wong, S.F., and Whitehouse, C.M. (1989) Electrospray ionization for mass spectrometry of large biomolecules. *Science* **246**, 64–71
18. Tanaka, K., Waki, H., Ido, H., Akita, S., and Yoshida T. (1988) Protein and polymer analyses up to m/z 100000 by laser ionization time-of-flight mass spectrometry. *Rapid. Commun. Mass Spectrom.* **2**, 151–153
19. Karas, M. and Hillenkamp, F. (1988) Laser desorption ionization of proteins with molecular masses exceeding 10, 000 daltons. *Anal. Chem.* **60**, 2299–2301
20. Yamamoto, T., Izumi, S., and Gekko, K. (2004) Mass spectrometry on segment-specific hydrogen exchange of dihydrofolate reductase. *J. Biochem.* **135**, 17–24
21. Yamamoto, T., Izumi, S., Ohmae, E., and Gekko, K. (2004) Mass spectrometry of hydrogen/deuterium exchange of *Escherichia coli* dihydrofolate reductase: Effects of loop mutations. *J. Biochem.* **135**, 487–494
22. Iwakura, M., Jones, B.E., Luo, J., and Matthews, C.R. (1995) A strategy for testing the suitability of cysteine replacements in dihydrofolate reductase from *Escherichia coli*. *J. Biochem.* **117**, 480–488
23. Fierke, C.A., Johnson, K.A., and Benkovic, S.J. (1987) Construction and evaluation of the kinetic scheme associated with dihydrofolate reductase from *Escherichia coli*. *Biochemistry* **26**, 4085–4092
24. Williams, E.A. and Morrison, J.F. (1991) Characterization of tightly bound substrates in pure preparations of dihydrofolate reductase: implications for studies on enzymes. *Biochim. Biophys. Acta* **1078**, 47–55
25. Kamiyama, T. and Gekko, K. (2000) Effect of ligand binding on the flexibility of dihydrofolate reductase as revealed by compressibility. *Biochim. Biophys. Acta* **1478**, 257–266
26. Takahashi, T., Nakanishi, M., and Tsuboi, M. (1978) Hydrogen-deuterium exchange rate between a peptide group and an aqueous solvent as determined by a stopped flow ultraviolet spectrophotometry. *Bull. Chem. Soc. Jpn.* **51**, 1988–1990
27. Miller, G.P. and Benkovic, S.J. (1998) Deletion of a highly motional residue affects formation of the Michaelis complex for *Escherichia coli* dihydrofolate reductase. *Biochemistry* **37**, 6327–6335
28. Miller, G.P. and Benkovic, S.J. (1998) Strength of an interloop hydrogen bond determines the kinetic pathway in catalysis by *Escherichia coli* dihydrofolate reductase. *Biochemistry* **37**, 6336–6342
29. Osborne, M.J., Schnell, J., Benkovic, S.J., Dyson, H.J., and Wright, P.E. (2001) Backbone dynamics in dihydrofolate reductase complexes: Role of loop flexibility in the catalytic mechanism. *Biochemistry* **40**, 9846–9859